

CoATA: Effective Co-Augmentation of Topology and Attribute for Graph Neural Networks

Tao Liu
College of Computer and
Information Science,
Southwest University
Chongqing, China
taoliu.swu@gmail.com

Longlong Lin
College of Computer and
Information Science,
Southwest University
Chongqing, China
longlonglin@swu.edu.cn

Yunfeng Yu
College of Computer and
Information Science,
Southwest University
Chongqing, China
YunfengYu817@outlook.com

Xi Ou
College of Computer and
Information Science,
Southwest University
Chongqing, China
xiou.cs@outlook.com

Youan Zhang
College of Computer and
Information Science,
Southwest University
Chongqing, China
youan0529@email.swu.edu.cn

Zhiqiu Ye
College of Computer and
Information Science,
Southwest University
Chongqing, China
zqiuye@outlook.com

Tao Jia
College of Computer and
Information Science,
Southwest University
Chongqing, China
tjia@swu.edu.cn

Abstract

Graph Neural Networks (GNNs) have garnered substantial attention due to their remarkable capability in learning graph representations. However, real-world graphs often exhibit substantial noise and incompleteness, which severely degrades the performance of GNNs. Existing methods typically address this issue through single-dimensional augmentation, focusing either on refining topology structures or perturbing node attributes, thereby overlooking the deeper interplays between the two. To bridge this gap, this paper presents CoATA, a dual-channel GNN framework specifically designed for the Co-Augmentation of Topology and Attribute. Specifically, CoATA first propagates structural signals to enrich and denoise node attributes. Then, it projects the enhanced attribute space into a node-attribute bipartite graph for further refinement or reconstruction of the underlying structure. Subsequently, CoATA introduces contrastive learning, leveraging prototype alignment and consistency constraints, to facilitate mutual corrections between the augmented and original graphs. Finally, extensive experiments on seven benchmark datasets demonstrate that the proposed CoATA outperforms eleven state-of-the-art baseline methods, showcasing its effectiveness in capturing the synergistic relationship between topology and attributes.

CCS Concepts

• **Computing methodologies** → **Machine learning algorithms**.

Keywords

Multimedia Machine Learning; Graph Neural Networks; Graph Augmentation

ACM Reference Format:

Tao Liu, Longlong Lin, Yunfeng Yu, Xi Ou, Youan Zhang, Zhiqiu Ye, and Tao Jia. 2025. CoATA: Effective Co-Augmentation of Topology and Attribute for Graph Neural Networks. In *Proceedings of the 2025 International Conference on Multimedia Retrieval (ICMR '25)*, June 30–July 3, 2025, Chicago, IL, USA. ACM, New York, NY, USA, 11 pages. <https://doi.org/10.1145/3731715.3733291>

1 Introduction

Graphs are foundational data structures for modeling relationships among entities in diverse real-world domains. Graph Neural Networks (GNNs) have emerged as a powerful paradigm to exploit such graph-structured data, driving advances in social media analysis [36, 46], recommender systems [18, 55], natural language processing [49, 50], and computer vision [22, 58]. Classical GNNs (e.g., GAT [43], GCN [24], and GraphSAGE [16]) and subsequent refinements [3, 5, 25, 51] maintain an embedding vector for each node, which is iteratively updated by aggregating the embeddings of its neighbors.

Despite their success, real-world graphs often suffer from significant noise and incompleteness, with corrupted topology structures and unreliable node attributes, which can severely degrade the performance of GNNs [9, 10, 30]. Therefore, numerous graph augmentation methods (Section 2) have been proposed to alleviate the issues mentioned above. However, existing methods typically focus on only one of these two aspects: (i) Topology-oriented methods, such as edge denoising [32], random walks [62], or auxiliary nodes [2], aim to repair structural gaps but often overlook the frequent attribute corruption. (ii) Attribute-oriented methods focus on feature-space enhancements, such as feature (i.e., attribute) masking [11], feature propagation [13], or feature mixup [17]. These techniques assume the underlying topology is sufficiently reliable to guide message passing or synthetic feature generation. Consequently, such *single-dimensional* approaches tend to create a dilemma loop: missing or incorrect edges impede effective feature propagation,

Permission to make digital or hard copies of all or part of this work for personal or classroom use is granted without fee provided that copies are not made or distributed for profit or commercial advantage and that copies bear this notice and the full citation on the first page. Copyrights for components of this work owned by others than the author(s) must be honored. Abstracting with credit is permitted. To copy otherwise, or republish, to post on servers or to redistribute to lists, requires prior specific permission and/or a fee. Request permissions from permissions@acm.org.
ICMR '25, Chicago, IL, USA

© 2025 Copyright held by the owner/author(s). Publication rights licensed to ACM.
ACM ISBN 979-8-4007-1877-9/2025/06
<https://doi.org/10.1145/3731715.3733291>

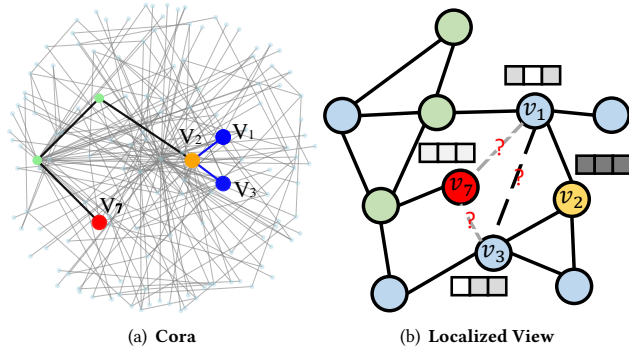


Figure 1: (a) Visualization of the Cora dataset, where nodes of the same class (v_2, v_7) are found to be multi-hop away. (b) A magnified subgraph where existing graph augmentation methods may fail to establish meaningful connections.

while noisy attributes mislead topology refinements, leading to ineffective learning in real-world graphs.

To illustrate, consider the widely used Cora dataset [39], a citation network where nodes represent research publications and edges indicate citation relationships (Fig.1). Due to the sparsity of direct citations or the high-dimensional and noisy nature of textual features, semantically similar papers may remain unlinked. For example, nodes v_1 and v_3 might be from the same cluster due to they share a neighbor v_2 . However, another node v_7 , despite belonging to the same class with v_2 , remains disconnected due to a missing direct citation link to v_2 and its multi-hop away from the core cluster. Thus, existing attribute-oriented methods suffer from two critical limitations. First, they only aggregate information from immediate neighbors, meaning that any missing or spurious edges can lead to significant information loss or contamination. Second, such local propagation mechanisms often lead to over-smoothing when stacking multiple layers, especially problematic in networks with noisy or heterophilic connections [4]. On the other hand, existing topology-oriented methods often use naive cosine similarity on node attributes to reweight edges also presents challenges. For example, the high-dimensional, sparse nature of the feature vectors means that direct cosine similarity is extremely sensitive to noise; even a few corrupted or missing features can drastically lower the similarity score between nodes that are semantically related in reality. As a consequence, for Fig.1, without effective feature propagation via an intermediary such as v_2 , nodes v_1 and v_3 would not exhibit a high cosine similarity based solely on their raw features. Furthermore, since the enriched features of v_2 fail to propagate to v_7 , the cosine similarity between v_7 and either v_1 or v_3 may collapse to nearly zero, completely masking their latent semantic relevance. Thus, designing the interplay between topology and attributes is both crucial and challenging for achieving robust graph learning.

To tackle the challenge above, we propose a novel framework, Co-Augmentation of Topology and Atttribute (CoATA), which consists of three principal components: the Topology-Enriched Attributes (TEA) module (Section 4.1), the Attribute-Informed Topology (AIT) module (Section 4.2), and Dual-Channel GNN with Prototype Alignment (DPA) module (Section 4.3). Unlike conventional augmentation techniques that separately enhance topology or attributes,

CoATA explicitly co-optimizes both through an iterative correction process. Specifically, while many conventional methods rely solely on the homophily assumption [31], our TEA module employs higher-order propagation via a residual mechanism to both strengthen local homophilic signals and mitigate the adverse effects of heterophilic or noisy connections. This step can correct or enrich local attributes (e.g., effectively bridging v_2 with v_1 and v_3) and even propagate informative signals to moderately distant nodes like v_7 ; However, not all nodes similar to v_7 or those even farther from the central hub can reliably receive the propagated information, as the reach of TEA remains limited. Hence, AIT constructs a node-attribute bipartite graph and leverages the celebrated proximity metric Personalized PageRank [26] to traverse multi-hop feature pathways on a global scale, forging new or refined edges (e.g., eventually connecting these distant nodes to the core cluster once partial overlaps accumulate). As a result, the co-augmented graph better reflects genuine node proximities than raw structural or naive attribute-based measures. Finally, since neither the original nor the augmented graph is perfect, DPA maintains both views in a dual-channel model, which retains raw edges while injecting the co-augmented structure. To ensure consistent class-level semantics, we devise a prototype-based contrastive loss, guiding both channels to converge on unified and robust representations. This synergy robustly combines local and global signals, mitigating any bias from a single dimension. In a nutshell, we highlight the main contributions as follows:

Co-Augmentation Pipeline. We present a novel approach that integrates *topology-enriched attributes* and *attribute-informed topology* into a unified framework. This bidirectional process leverages higher-order structural cues to clean attributes and then uses the improved features to correct or supplement the adjacency matrix.

Dual-Channel GNN with Prototype Alignment. We propose a dual-channel GNN that preserves both the original and the augmented adjacency matrices. We devise a prototype-based contrastive loss to ensure consistent class-level semantics, guiding both channels to converge on unified and robust representations.

Extensive Experiments. We conduct extensive experiments on seven real-world graphs and eleven baselines to validate the effectiveness of our solutions. The results show that the proposed CoATA consistently outperforms most existing augmentation methods, achieving accuracy improvements ranging from 1.1% to 17.9%.

2 Related Work

Topology-oriented Augmentation techniques aim to enhance GNNs performance through structural modifications that address incomplete or noisy graph connectivity [30]. Early approaches relied on stochastic edge manipulation, with methods like DropEdge [37] demonstrating that random edge removal could effectively regularize GNNs and alleviate over-smoothing issues [4]. Subsequent research has evolved toward more sophisticated structural adaptation strategies, which can be broadly categorized into three paradigms: (i) *Similarity-based methods* leverage node similarity metrics to guide structural modifications. Works such as

[7, 20, 32, 54, 62] compute pairwise node similarities to dynamically adjust edge connections, thereby better capturing latent relational patterns through adaptive topology refinement. (ii) *Graph regeneration approaches* employ generative models to reconstruct graph structures. Techniques including [14, 34, 40, 45, 59] utilize graph autoencoders [23] and stochastic block models [19] to learn edge formation dynamics, generating synthetic topologies that preserve critical structural properties. (iii) *Global and high-order augmentation* focus on augmenting graph structure by incorporating global connectivity information or higher-order substructures. For instance, S³-CL [8] employs structure and semantic contrastive learning to enhance global topology awareness. GloGNN [27] utilizes the global adjacency matrix to transcend local neighborhood limitations. PSA-GNN [53] introduces high-order subgraphs (e.g., motifs, cliques), thus extending standard node-level connectivity to richer topological constructs.

Attribute-oriented Augmentation techniques enhance GNNs performance through feature-space modifications, primarily employing three strategies: feature masking, feature propagation, and feature mixup. Feature masking [42, 61] randomly obscures feature dimensions during training to prevent over-reliance on specific attributes. For example, DropMessage [11] extends traditional dropout by probabilistically masking message matrix elements, enabling fine-grained regularization. Feature propagation [8, 12, 30] iteratively aggregates neighborhood features to construct noise-resistant representations that capture structural context. For example, GRAND [13] leverages multiple feature propagation to create diverse augmented graphs, exposing models to varied structural contexts for improved robustness. SimP-GCN [21] focuses on preserving original feature similarity to prevent distortions during message passing. By constraining the extent of information propagation, SimP-GCN mitigates over-smoothing and retains critical attribute-level distinctions. Feature mixup [15, 17, 44] generates synthetic samples through convex feature combinations, improving model generalizability. For example, GeoMix [60] integrates mixup operations within propagation steps, generating interpolated features that preserve topological smoothness.

3 Preliminaries

Basic Notations. Given an undirected and unweighted graph $G = (V, E)$, where V represents the node set with $n = |V|$ nodes, and E denotes the edge set with $m = |E|$ edges. We define the adjacency matrix $\mathbf{A} \in \{0, 1\}^{n \times n}$. Namely, $\mathbf{A}_{uv} = 1$ if $(u, v) \in E$; otherwise, $\mathbf{A}_{uv} = 0$. Furthermore, each node $u \in V$ is endowed with an attribute (feature) vector $\mathbf{x}_u \in \mathbb{R}^k$, and the collection of these attribute vectors forms the node attribute matrix $\mathbf{X} = [\mathbf{x}_1^T; \mathbf{x}_2^T; \dots; \mathbf{x}_n^T] \in \mathbb{R}^{n \times k}$, where k signifies the dimensionality of the features. Besides, let $N(u) = \{v \mid (u, v) \in E\}$ be the neighbors of node u . We introduce the degree diagonal matrix $\mathbf{D} \in \mathbb{R}^{n \times n}$, which is defined as $\mathbf{D} = \text{diag}(d(u_1), d(u_2), \dots, d(u_n))$, where $d(u_i) = |N(u_i)|$ represents the degree of node u_i . To facilitate our discussion, we partition the node set V into two subsets: \mathcal{V}_l and \mathcal{V}_u , where \mathcal{V}_l contains the labeled nodes, and $\mathcal{V}_u = V \setminus \mathcal{V}_l$ consists of the unlabeled nodes. Our primary goal is to leverage the information provided by the labeled nodes \mathcal{V}_l to predict the labels of the unlabeled nodes \mathcal{V}_u .

Graph Neural Network (GNN) is a specialized neural network architecture designed for handling graph-structured data [16, 24, 33, 43, 56], which aims to map nodes into low-dimensional embedding vectors, capturing both the topology structures and node attributes. GNN regulates the spread and update of information through defined node aggregation and update functions, allowing nodes to integrate information from their neighboring nodes and refine their own embedding vectors. This iterative process persists until the model convergence: $h_u^{(l+1)} = \text{UPDATE}(h_u^{(l)}, \text{AGGREGATE}(h_v^{(l)} \mid v \in N(u)))$, where $h_u^{(l)}$ represents the embedding of node u at layer l . The AGGREGATE(\cdot) function assigns weights to the embeddings of neighboring nodes v relative to node u . The UPDATE(\cdot) function iteratively refines the features of all nodes based on the aggregated information. Among the various GNN models, the Graph Convolutional Network (GCN) [24] is ubiquitous, which is stated as follows:

$$\mathbf{H}^{(l+1)} = \sigma\left(\tilde{\mathbf{A}}\mathbf{H}^{(l)}\mathbf{W}^{(l)}\right), \quad l = 0, 1, \dots \quad (1)$$

Here, $\mathbf{H}^{(l)}$ denotes the node embedding matrix at layer l , with $\mathbf{H}^{(0)} = \mathbf{X}$. The propagation matrix $\tilde{\mathbf{A}} = \hat{\mathbf{D}}^{-1/2}\hat{\mathbf{A}}\hat{\mathbf{D}}^{-1/2}$ is derived from the adjacency matrix \mathbf{A} , where $\hat{\mathbf{A}} = \mathbf{A} + \mathbf{I}$, $\hat{\mathbf{D}} = \mathbf{D} + \mathbf{I}$, and \mathbf{I} is the identity matrix. $\mathbf{W}^{(l)}$ represents the trainable weight matrix at layer l , and $\sigma(\cdot)$ is the activation function (e.g., ReLU).

Personalized PageRank (PPR) is the cutting-edge proximity metric that measures the relative importance of nodes [1, 28, 29]. The PPR value $\Pi(u, v)$ represents the probability that an α -decay random walk starting from node u stops at node v . In an α -decay random walk, there is an α probability of stopping at the current node or a $(1 - \alpha)$ probability of randomly jumping to one of its neighbors. Consequently, the length of an α -decay random walk follows a geometric distribution with a success probability of α . Therefore, the PPR matrix Π can capture the higher-order proximity, which is formulated as follows:

$$\Pi = \sum_{r=0}^{\infty} \alpha(1 - \alpha)^r \cdot \mathbf{P}^r \quad (2)$$

where \mathbf{P} is the state transition matrix, typically set to $\mathbf{D}^{-1}\mathbf{A}$.

4 COATA: The Proposed Solution

We propose a dual-channel approach *CoATA* for Co-Augmentation of Topology and Attribute (Fig. 2). Specifically, *CoATA* first utilizes the Topology-Enriched Attribute (*TEA*) module to incorporate higher-order structural signals, thereby refining and denoising node features (Section 4.1). Next, the enriched features construct a bipartite graph, and the Attribute-Informed Topology (*AIT*) module applies the PPR metric to this bipartite graph to more effectively capture multi-hop indirect relationships between nodes (Section 4.2). Finally, *CoATA* unifies the raw and augmented graphs through Dual-Channel GNN with Prototype Alignment (*DPA*), ensuring that node embeddings derived from the raw and augmented views remain consistent (Section 4.3).

4.1 Topology-Enriched Attribute Augmentation

Real-world graphs often exhibit noisy or incomplete connections and may also be *heterophilic* [31], meaning that directly connected nodes can belong to different classes. In such cases, relying solely

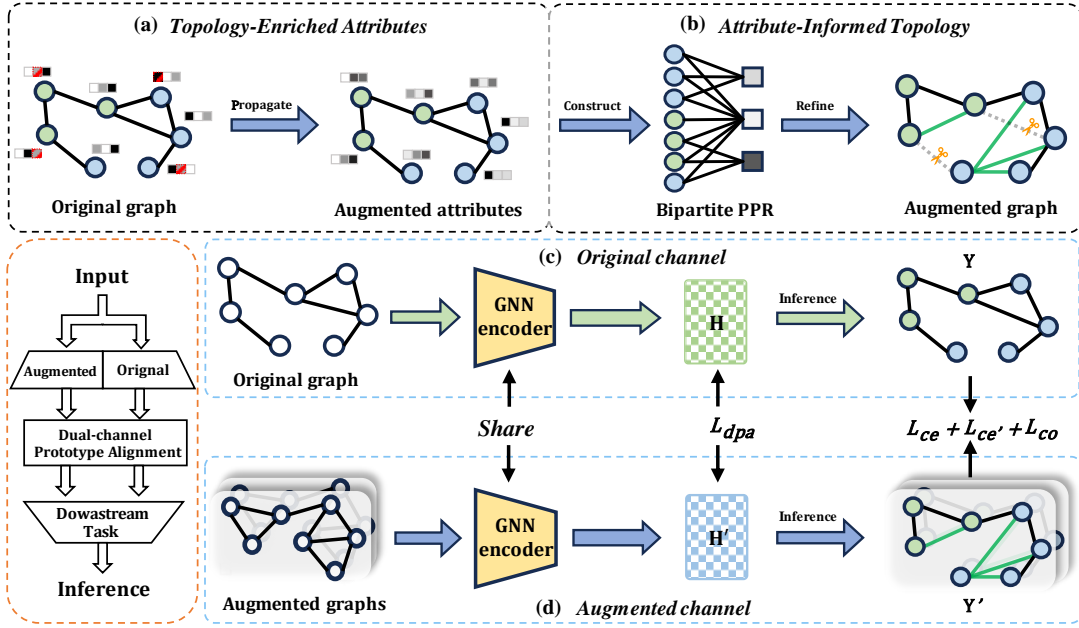


Figure 2: The framework of CoATA. (a) TEA improves node features via *higher-order propagation*; (b) AIT refines graph structure through a *node-attribute bipartite graph*. The model has two channels: (c) Original channel processes the raw graph; (d) Augmented channel leverages the co-augmented graph. Both share a GNN encoder, with DPA ensuring cross-view consistency. Supervised losses ($L_{ce} + L'_{ce}$) guide label predictions, and consistency loss (L_{co}) aligns outputs across augmented graphs.

on single-hop neighbors for message passing can lead to feature contamination and insufficient representation. To address this issue, we propose a higher-order augmentation method that leverages multi-hop structural signals. By propagating node attributes over multiple steps, distant but semantically relevant information is incorporated, helping to overcome local inconsistencies or missing edges. This process lays a robust foundation for subsequent stages in our co-augmentation pipeline, especially when the graph structure is imperfect or deviates from traditional homophily assumptions.

Higher-order Attribute Propagation. We iteratively propagate the attribute matrix X over a normalized adjacency matrix \tilde{A} . Let $X^{(0)} = X$ denote the initial feature matrix. At each l -th propagation step, we compute:

$$X^{(l)} = \tilde{A} X^{(l-1)}. \quad (3)$$

However, propagating through too many hops may lead to over-mixing of features, especially in heterophilic graphs where local neighborhoods can be misleading. To preserve node-specific information, we incorporate a residual mixing mechanism [6] controlled by the residual coefficient $\beta \in [0, 1]$:

$$X^{(l)} = (1 - \beta) \tilde{A} X^{(l-1)} + \beta X, \quad (4)$$

Algorithm 1 summarizes the procedure of *Topology-Enriched Attribute Augmentation*, demonstrating how to integrate higher-order information while retaining node-specific features.

THEOREM 4.1 (HETEROPHILY ALLEVIATION VIA RESIDUAL PROPAGATION [60]). Consider a heterophilic graph with C classes, where each node u has a class label y_u . Let μ_c denote the mean feature vector

Algorithm 1 Topology-Enriched Attribute Augmentation

Input: Node feature matrix $X \in \mathbb{R}^{n \times k}$, normalized adjacency matrix $\tilde{A} \in \mathbb{R}^{n \times n}$, residual coefficient $\beta \in [0, 1]$, propagation steps h .
Output: Enriched node feature matrix $H \in \mathbb{R}^{n \times k}$.

- 1: $X^{(0)} \leftarrow X$;
- 2: **for** $l = 1$ to h **do**
- 3: $X' \leftarrow \tilde{A} \cdot X^{(l-1)}$ // Aggregate multi-hop neighbor features
- 4: $X^{(l)} \leftarrow (1 - \beta) \cdot X' + \beta \cdot X$ // Residual mixing
- 5: **end for**
- 6: **return** $H \leftarrow X^{(h)}$.

of class c . Suppose the node feature update follows Eq. (4). Let

$$p_0 \approx \mathbb{P}(y_v = y_u \mid v \in \mathcal{N}(u))$$

indicate the heterophily level (with lower p implying stronger heterophily). Then, after l propagation steps, the expected feature representation of node u is

$$\mathbb{E}[x_u^{(l)}] = p_l \mu_{y_u} + (1 - p_l) \sum_{c \neq y_u} \frac{1}{C-1} \mu_c, \quad (5)$$

where $p_l = \beta + (1 - \beta) p_{l-1}$. As $l \rightarrow \infty$, we have $p_l \rightarrow 1$. Thus, the residual propagation progressively amplifies the influence of the correct class center μ_{y_u} , thereby mitigating feature contamination from heterophilic neighbors.

PROOF. Since the proof of this theorem directly comes from [60], we omit it for brevity. \square

Balancing Propagation and Feature Retention. Although multi-hop propagation can expand a node's receptive field and capture global signals, the parameter β in Eq. (4) limits the amount of new

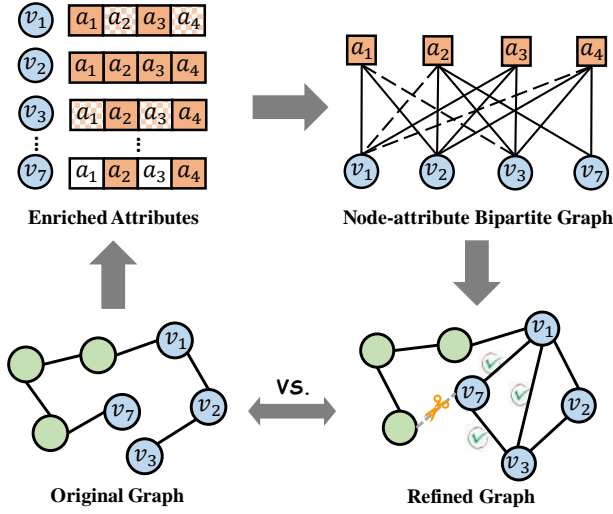


Figure 3: Nodes v_1, v_2, v_3, v_7 share the same class. AIT connects distant nodes (e.g., v_7) via multi-hop feature walks.

information integrated at each step. As indicated in Theorem 4.1, this residual mixing gradually strengthens the alignment with the correct class center, thereby mitigating feature contamination from dissimilar neighbors. This prevents oversmoothing, where nodes of different classes become too similar, but it also sets a limit on how far multi-hop expansion can reach when certain subgraphs are disconnected. In Fig. 1, nodes v_1 and v_3 are directly connected to v_2 , so multi-hop propagation allows them to share partial attributes. However, other nodes such as v_7 that are several hops away from v_2 is difficult to effectively enriched by TEA. Consequently, TEA helps some nodes discover shared features (e.g., \mathbf{x}_{v_1} and \mathbf{x}_{v_3}), but more distant nodes with no bridging path may also remain overlooked.

4.2 Attribute-informed Topology Augmentation

After obtaining topology-enriched attributes (Section 4.1), we further leverage them to refine the original graph structure. Although node features often contain valuable clues about node similarity, traditional distance metrics (e.g., Cosine or Euclidean) can fail under noise or sparsity, especially for pairs of nodes that are multi-hop away. For example, in Fig. 3, nodes v_1 and v_3 might be recognized as similar after TEA, yet v_7 being too distant from v_2 , still remains disconnected. A simple cosine measure on $\{\mathbf{x}_{v_1}, \mathbf{x}_{v_7}\}$ could report near-zero overlap if their local features have not been sufficiently propagated. To address this shortfall, we propose constructing a *node-attribute bipartite graph* and applying the well-known proximity metric PPR to it, thus capturing indirect multi-hop attribute relationships from a *global perspective*. As a result, nodes can connect via shared feature dimensions even if they reside in different parts of the original graph.

Node-attribute Bipartite Graph Construction. Let $\mathbf{H} \in \mathbb{R}^{n \times k}$ be the enriched node-feature matrix by TEA (Algorithm 1) in Section 4.1. We construct the node-attribute bipartite graph as follows (Fig. 3). Let $G_b = (U \cup V, E_b)$ be a bipartite graph, in which $U = \{a_1, a_2, \dots, a_k\}$ is the attribute set and $V = \{v_1, v_2, \dots, v_n\}$ is the node set of the original input graph G . The edge set $E_b \subseteq U \times V$ and each edge $(a_i, v_j) \in E_b$ is associated with a non-negative weight

$w(a_i, v_j) = H_{ij}$. To ensure the robustness of attribute information and prevent spurious signals from negatively impacting similarity computations in practice, we preprocess the feature matrix \mathbf{H} using the following procedure: (i) Zero-Dimension Removal: Remove any feature dimension (i.e., column) that is entirely zero across all nodes. (ii) Singleton Filtering: Optionally filter or down-weight feature dimensions that are nonzero for only a single node, since these features do not contribute to similarity between nodes. By projecting the enriched feature matrix \mathbf{H} into this bipartite graph, random walks can move from an attribute a_i to a node v_j if $H_{ij} \neq 0$, thereby capturing latent attribute overlaps. The bipartite construction can effectively model such relationships, even in the presence of noise or missing features.

Push-based PPR on Bipartite Graphs. Since conventional similarity metrics, such as cosine or Euclidean distance, often struggle to capture indirect relationships in the presence of sparse or noisy node features [21], we instead adopt the PPR metric, which effectively captures multi-hop connectivity within the feature space. Recall that PPR on a graph $G = (V, E)$ with adjacency matrix \mathbf{A} is defined as the unique stationary distribution $\boldsymbol{\pi}$ satisfying:

$$\boldsymbol{\pi} = \alpha \mathbf{e}_s + (1 - \alpha) \boldsymbol{\pi} \mathbf{D}^{-1} \mathbf{A}, \quad (6)$$

where \mathbf{e}_s is a one-hot vector indicating the source node s , $\alpha \in (0, 1)$ is the teleportation probability, and \mathbf{D} is the diagonal degree matrix. Note that Eq. (6) is a variant of Eq. (2) [1].

However, PPR is designed for general unipartite graphs and does not inherently consider the distinctive properties of bipartite graphs. When applied to the bipartite graph G_b , it generates distributions over both U and V . To address this limitation, we propose a novel and efficient push-based strategy (Algorithm 2) that retains the final PPR scores exclusively within V , which is our significant technical contribution. Specifically, the procedure initializes the approximate PPR and residue vectors as $\hat{\boldsymbol{\pi}}_s = \mathbf{0}$ and $\mathbf{r}_s = \mathbf{e}_s$ (Line 1). It then performs forward-push operations on nodes v that satisfy the condition $\frac{\mathbf{r}_s(v)}{d(v)} > r_{\max}$ (Lines 2-3). Here, r_{\max} serves as a parameter that balances the trade-off between the precision and computational efficiency of the PPR computation. During each push operation, a fraction α of the residue is retained, while the remaining $1 - \alpha$ is propagated to neighboring nodes (Lines 5-8). Once all neighbors of v have been updated, the residue $\mathbf{r}_s(v)$ is reset to zero (Line 4). Subsequently, the residues accumulated at nodes in $N(v)$ are pushed back to V , ensuring no residue loss (Lines 9-14). The algorithm terminates once all nodes $v \in V$ meet $\frac{\mathbf{r}_s(v)}{d(v)} \leq r_{\max}$.

Remark. This reconstruction process (Algorithm 2) benefits from the enriched features in Section 4.1, since multi-hop residual propagation already reduces local inconsistencies. Hence, the push-based PPR on the bipartite graph can further uncover *global* relationships through cross-feature walks. Even if certain nodes are only partially corrected by TEA, bipartite PPR can connect them to more suitable neighbors. Moreover, Theorem 4.2 provides a lower bound on bipartite PPR scores for nodes reachable via length- $2c$ paths, ensuring these multi-hop connections are not overlooked. This approach overcomes the sparsity of direct similarity measures, revealing high-order attribute links beyond local structural limits.

Algorithm 2 Intra-Set Forward Push over Bipartite Graphs

Input: Bipartite graph $G_b = (U \cup V, E_b)$, source node $s \in V$, teleportation probability α , threshold r_{max} .

Output: $\{\hat{\pi}_s(v) \mid v \in V\}$.

```

1:  $\hat{\pi}_s \leftarrow \mathbf{0}, r_s \leftarrow e_s;$ 
2: while  $\exists v \in V$  s.t.  $\frac{r_s(v)}{d(v)} > r_{max}$  do
3:   pick an arbitrary node  $v$  with  $\frac{r_s(v)}{d(v)} > r_{max}$ ;
4:    $r \leftarrow r_s(v), r_s(v) \leftarrow 0;$ 
5:    $\hat{\pi}_s(v) \leftarrow \hat{\pi}_s(v) + \alpha \cdot r;$ 
6:   for  $u \in N(v)$  do
7:      $r_s(u) \leftarrow r_s(u) + \frac{(1-\alpha) \cdot w(u,v)}{\sum_{u_i \in N(v)} w(u,u_i)} \cdot r;$ 
8:   end for
9:   for  $u \in N(v)$  do
10:     $r \leftarrow r_s(u), r_s(u) \leftarrow 0;$ 
11:    for  $v_i \in N(u)$  do
12:       $r_s(v_i) \leftarrow r_s(v_i) + \frac{w(v_i,u)}{\sum_{v \in N(u)} w(v,u)} \cdot r;$ 
13:    end for
14:  end for
15: end while
16: return  $\{\hat{\pi}_s(v) \mid v \in V\};$ 

```

THEOREM 4.2 (BIPARTITE-PPR LOWER BOUND). *For any node v_j reachable from s by a length- $2c$ path in G_b ,*

$$\pi_s(v_j) \geq \alpha(1-\alpha)^{2c} |\mathcal{P}_{2c}(s \rightsquigarrow v_j)| \left(\frac{w_{\min}^2}{d_{\max}^2 d_{\max}} \right)^c.$$

PROOF. The detailed proof of the theorem is put in our Supplementary Material due to the space limits. \square

Co-Augmented Global Graph Reconstruction. After obtaining node-level PPR scores $\hat{\pi}_{ij}$ among nodes in V , a new Co-Augmented global adjacency matrix $\tilde{\mathbf{A}}^{(c)}$ can be reconstructed using two flexible strategies: ① Fixed-size KNN Graph: This method selects a global K such that the resulting graph has a comparable number of edges to the original. For each node v_i , the top- K neighbors v_j with the highest $\hat{\pi}_{ij}$ values are selected to form edges in the new adjacency matrix. ② Edge Addition/Removal: Alternatively, the original adjacency matrix can be incrementally modified based on the PPR ranking. For each node, edges are selectively added or removed based on their PPR ranking. A fixed number of edges can be added or removed per node (e.g., k_{add} , k_{del}) to update the original adjacency matrix.

Overall, by combining the enriched attributes (Section 4.1) with the bipartite PPR process here, we achieve a robust co-augmentation frame that captures both localized and global signals, effectively mitigating noise or partial inconsistencies in real-world graphs.

4.3 Dual-Channel GNN with Alignment

Having introduced two complementary graph views in Sections 4.1 and 4.2, we now unify them using a dual-channel scheme. The original adjacency matrix $\tilde{\mathbf{A}}$ retaining raw but possibly noisy edges, thereby preserving faithful local patterns. In contrast, the refined adjacency matrix $\tilde{\mathbf{A}}^{(c)}$ derived via bipartite PPR, captures broader global connectivity that may be missed by the original graph alone.

Dual-Channel Model Setup. We employ a single GNN architecture with *shared* parameters across both channels. The original channel processes $(\tilde{\mathbf{A}}, \mathbf{X})$, while the co-augmented channel takes

$(\tilde{\mathbf{A}}^{(c)}, \mathbf{X})$, producing:

$$\hat{\mathbf{Y}} = \text{GNN}(\tilde{\mathbf{A}}, \mathbf{X}), \quad \hat{\mathbf{Y}}' = \text{GNN}(\tilde{\mathbf{A}}^{(c)}, \mathbf{X}), \quad (7)$$

By sharing weights, we reduce the overall number of parameters and encourage robustness across both original and augmented structures. Each channel is supervised with a cross-entropy term:

$$\mathcal{L}_{ce} = - \sum_{i \in \mathcal{V}_I} Y(i) \log \hat{Y}(i), \quad \mathcal{L}'_{ce} = - \sum_{i \in \mathcal{V}_I} Y(i) \log \hat{Y}'(i), \quad (8)$$

Where $Y(i)$ denotes the label for node i , and \mathcal{V}_I is the training set.

Consistency Across Multiple Augmentations. In practice, we construct two specific augmented graphs $\tilde{\mathbf{A}}^{(c)}$: one using the Fixed-size KNN Graph strategy and the other using the Edge Addition and Removal strategy (see Section 4.2). To ensure coherence and leverage both augmented graphs effectively, we adopt a consistency loss that aligns the model's outputs.

$$\mathcal{L}_{co} = \frac{1}{S} \sum_{s=1}^S \sum_{i \in V} \left\| \mathbf{Y}^{\text{agg}}(i) - \hat{\mathbf{Y}}'_s(i) \right\|_2^2, \quad (9)$$

where $\hat{\mathbf{Y}}'_s$ denotes the augmented-channel predictions under the s -th augmented adjacency matrix, and $\mathbf{Y}^{\text{agg}}(i)$ is an aggregated pseudo-label [38] (e.g., averaged predictions). This term encourages outputs to remain consistent across different $\tilde{\mathbf{A}}^{(c)}$.

Dual-Channel Prototype Alignment. Even if the augmented graphs are consistent internally, they may still diverge from the original adjacency matrix in terms of class-level semantics. Inspired by [52, 57], we impose a *prototype alignment* to align embeddings across channels. Let $\mathbf{Z}, \mathbf{Z}' \in \mathbb{R}^{n \times d}$ be the hidden embeddings for the original and augmented channels, respectively. For class $j \in \{1, \dots, C\}$, we define:

$$\mathbf{p}_j = \frac{\sum_{i: \arg \max \hat{Y}_{i=j}} t_i \mathbf{Z}_i}{\sum_{i: \arg \max \hat{Y}_{i=j}} t_i}, \quad \mathbf{p}'_j = \frac{\sum_{i: \arg \max \hat{Y}'_{i=j}} t_i \mathbf{Z}'_i}{\sum_{i: \arg \max \hat{Y}'_{i=j}} t_i}, \quad (10)$$

where t_i is a confidence weight (1 if labeled, or the highest predicted probability if unlabeled). We then adopt a contrastive loss:

$$\mathcal{L}_{dpa} = -\frac{1}{2c} \sum_{j=1}^c \left(\log \frac{f(\mathbf{p}_j, \mathbf{p}'_j)}{\sum_{q \neq j} f(\mathbf{p}_j, \mathbf{p}'_q)} + \log \frac{f(\mathbf{p}_j, \mathbf{p}'_j)}{\sum_{q \neq j} f(\mathbf{p}_q, \mathbf{p}'_j)} \right), \quad (11)$$

with $f(\mathbf{u}, \mathbf{v}) = e^{\cos(\mathbf{u}, \mathbf{v})/\tau}$, where τ is typically set to 0.5. This alignment pulls prototypes of the same class closer and pushes apart those from different classes, improving semantic consistency and reducing label mismatch [47], as stated in the following theorem.

THEOREM 4.3 (PROTOTYPE ALIGNMENT GUARANTEE). *Minimizing the contrastive loss \mathcal{L}_{dpa} ensures that prototypes from the same class across channels are pulled closer and those from different classes remain separated.*

PROOF. The detailed proof of the theorem is put in our Supplementary Material due to the space limits. \square

Overall Objective. We combine all the above loss components:

$$\mathcal{L} = \mathcal{L}_{ce} + \lambda_1 \mathcal{L}'_{ce} + \lambda_2 \mathcal{L}_{co} + \lambda_3 \mathcal{L}_{dpa}, \quad (12)$$

where $\lambda_1, \lambda_2, \lambda_3$ modulate the trade-off among supervision, inter-augmentation consistency, and cross-channel alignment.

Table 1: Statistics of datasets.

Dataset	#Nodes	#Edges	#Classes	#Features
Cora	2,708	5,429	7	1,433
CiteSeer	3,327	4,732	6	3,703
PubMed	19,717	44,338	3	500
Coauthor-CS	18,333	163,788	15	6,805
Coauthor-Phy	34,493	495,924	5	8,415
Chameleon	2,277	36,101	5	2,325
squirrel	5,201	217,073	5	2,089

5 Empirical Results

5.1 Experimental Setup

Datasets. We evaluate our solutions on seven standard graph benchmarks (Table 1): three citation networks (Cora, CiteSeer, PubMed [39]), two co-authorship networks (Coauthor-CS, Coauthor-Phy [41]), and two heterophilic graphs (Squirrel, Chameleon [35]). For citation networks, we adopt the data splits of [39], using 20 labeled nodes per class for training, 500 for validation, and 1000 for testing. For co-authorship networks, we follow [41] with 20 labeled nodes per class for training, 30 for validation, and the rest for testing. For Squirrel and Chameleon, we follow the recent work [35] which filters out the overlapped nodes in the original datasets and uses its provided data splits. A detailed description of datasets is put in our Supplementary Material due to the space limits.

Baselines. We compare our proposed solutions with eleven competitors, which are summarized into three groups as follows. (1) Vanilla: GCN [24], GAT [43], SGC [51], and APPNP [25]; (2) Topology-oriented: S³-CL [8], GloGNN [27], and PSAGNN [53]; (3) Attribute-oriented: Mixup [48], Geomix [60], GraphMix [44], and Simp-GCN [21]. To mitigate the impact of randomness, we repeat each method five times and report the average value as the final performance.

Parameters and Implementations. Unless stated otherwise, we use the corresponding default parameters for all baselines. For our model, the key hyperparameters are α , β , and h , which are set within the ranges α in [0.1, 0.9], β in [0.1, 0.9], and h in [1, 4]. Our implementation uses Python, with DGL and PyG as the primary libraries. Our Supplementary Material provides further implementation details. All experiments are conducted on an Ubuntu 22.04.3 machine equipped with an NVIDIA RTX 4000 GPU, an Intel Xeon(R) 2.20GHz CPU, and 320GB of RAM.

5.2 Effectiveness Evaluation

Table 2 compares CoATA with 11 baselines on seven datasets. On homophilous datasets, we have the following observations: (1) CoATA achieves the best performance on four of five homophilous datasets. For example, on *Coauthor-Phy*, our CoATA attains 95.12%, surpassing all competitors by at least 0.56%. (2) On *PubMed*, CoATA ranks third and slightly behind the champion Simp-GCN. One possible reason is the relatively low-dimensional features in *PubMed* curtail the TEA’s ability to enhance noisy attributes. On the two heterophilic datasets *Squirrel* and *Chameleon*, we have the following observations. (1) Most topology-centric baselines fail to surpass even a plain GCN, indicating that naive structural modifications

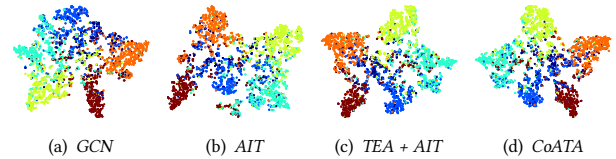


Figure 4: Visualization of our model CoATA. Nodes are colored by their corresponding labels.

can inadvertently reinforce mismatched neighbors. (2) CoATA outperforms all competitors by at least 1.31% and 1.40%, respectively, confirming that its dual-channel architecture effectively addresses *heterophily*. Overall, CoATA is consistently top on both graph types.

5.3 Ablation Studies

Table 3 shows the performance of each CoATA module on two homophilous datasets *Citeseer* and *CoAuthor-CS*, and one heterophilic dataset *Chameleon*. Other datasets behave similarly and are omitted for brevity. The theoretical rationale behind O_1 (*AIT*) is to refine the graph structure via adjacency augmentation; however, its modest gain (e.g., only +0.09% on *Citeseer*) indicates that structural enhancement alone is insufficient, especially in sparsely connected graphs that highlight the need for attribute enrichment. Incorporating O_2 (*TEA*) facilitates multi-hop neighbor signal propagation and mitigates local feature noise, a claim corroborated by the marked accuracy improvement observed on *Citeseer* (+3.92%), which aligns with our theoretical expectation that deeper neighborhood interactions strengthen feature propagation. The further addition of O_3 (*DPA*) introduces prototype alignment to reconcile raw and augmented representations, yielding the largest performance boost (+4.39%), and confirming that aligning multi-view representations is a key to overcoming systematic biases. Moreover, the significant drops observed when omitting consistency regularization (w/o \mathcal{L}_{co}) or the augmented-channel supervision (w/o \mathcal{L}'_{ce}) further emphasize the theoretical premise that integrated multi-view learning is crucial for improving performance.

5.4 Visualization of our model CoATA

Fig. 4 visualizes the embedding vectors learned by different methods on the *Citeseer* dataset, with similar trends observed across other datasets, which we omit for brevity. As can be seen, in Fig. 4(a), Vanilla GCN struggles to separate classes, as it aggregates disparate labels due to the limitations of one-hop propagation. In Fig. 4(b), *AIT* tightens clusters, yet some label overlap persists, highlighting the need for more nuanced feature propagation. In Fig. 4(c), with the introduction of *TEA* combined with *AIT*, multi-hop feature propagation further sharpens the decision boundaries, reducing label mixing. Finally, the full CoATA model in Fig. 4(d) achieves the sharpest and most distinct class separation, demonstrating how *DPA* resolves residual ambiguities by aligning node embeddings at the class level, leading to clearer decision boundaries.

5.5 Hyperparameter Analysis

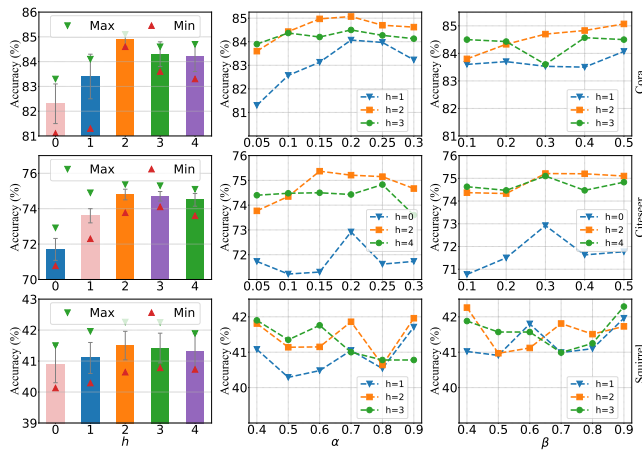
Fig. 5 illustrates the impact of three core hyperparameters in CoATA, focusing on α (teleportation probability in *AIT*), β (residual mixing coefficient in *TEA*), and h (propagation depth from Algorithm 1).

Table 2: Node classification accuracy (%). Each result is presented as the average \pm standard deviation, with the best result highlighted in bold.

Type	Method	Cora	PubMed	Citeseer	Coauthor-CS	Coauthor-Phy	Squirrel	Chameleon
Vanilla	GCN	81.63 \pm 0.45	78.88 \pm 0.65	70.98 \pm 0.37	91.16 \pm 0.52	92.85 \pm 1.03	39.47 \pm 1.47	40.89 \pm 4.12
	GAT	82.98 \pm 0.88	78.58 \pm 0.52	72.20 \pm 0.99	90.57 \pm 0.37	92.70 \pm 0.58	35.96 \pm 1.73	39.29 \pm 2.84
	SGC	80.35 \pm 0.24	78.75 \pm 0.17	71.87 \pm 0.14	90.37 \pm 1.01	92.80 \pm 0.15	39.04 \pm 1.92	39.35 \pm 2.82
	APPNP	83.33 \pm 0.52	79.78 \pm 0.66	71.83 \pm 0.52	91.97 \pm 0.33	93.86 \pm 0.33	37.64 \pm 1.63	38.25 \pm 2.83
Topology	S ³ -CL	84.83 \pm 0.21	80.73 \pm 0.28	74.97 \pm 0.52	91.29 \pm 0.17	93.26 \pm 0.42	38.13 \pm 1.36	40.33 \pm 3.21
	GloGNN	82.31 \pm 0.42	79.83 \pm 0.21	72.16 \pm 0.64	90.82 \pm 0.45	92.79 \pm 0.67	35.77 \pm 1.32	26.17 \pm 4.33
	PSAGNN	82.91 \pm 0.79	79.39 \pm 1.25	71.18 \pm 0.32	90.52 \pm 0.32	92.67 \pm 0.59	37.82 \pm 1.12	40.23 \pm 3.42
Attribute	Mixup	81.84 \pm 0.94	79.16 \pm 0.49	72.20 \pm 0.95	91.36 \pm 0.37	93.89 \pm 0.49	37.95 \pm 1.52	39.56 \pm 3.13
	GeoMix	84.22 \pm 0.85	80.18 \pm 0.99	75.12 \pm 0.26	92.23 \pm 0.14	94.56 \pm 0.06	40.95 \pm 1.12	42.67 \pm 2.44
	GraphMix	83.80 \pm 0.62	79.38 \pm 0.39	74.28 \pm 0.45	91.89 \pm 0.36	94.32 \pm 0.28	38.41 \pm 1.36	41.75 \pm 3.51
	Simp-GCN	82.83 \pm 0.26	80.84 \pm 0.17	72.63 \pm 0.59	90.54 \pm 0.45	93.43 \pm 0.54	39.26 \pm 1.87	40.93 \pm 4.25
This paper	CoATA	85.07 \pm 0.31	80.21 \pm 0.16	75.37 \pm 0.21	92.31 \pm 0.29	95.12 \pm 0.27	42.26 \pm 1.31	44.07 \pm 4.40

Table 3: Ablation Studies. O_1 refers to AIT, O_2 represents TEA, and O_3 denotes DPA. *w/o* means without.

Datasets	Citeseer	Coauthor-CS	Chameleon
GCN	70.98 \pm 0.37	91.16 \pm 0.52	40.89 \pm 4.12
O_1	71.07 \pm 0.45	91.84 \pm 0.45	42.11 \pm 4.52
$O_1 + O_2$	74.90 \pm 0.16	92.01 \pm 0.35	42.63 \pm 4.42
$O_1 + O_2 + O_3$	75.37 \pm 0.21	92.31 \pm 0.29	44.07 \pm 4.40
<i>w/o</i> \mathcal{L}_{co}	72.60 \pm 0.43	91.22 \pm 0.43	42.66 \pm 4.18
<i>w/o</i> \mathcal{L}'_{ce}	72.80 \pm 0.24	90.53 \pm 0.24	40.37 \pm 4.42

**Figure 5: Hyperparameter Analysis.** Left bar charts depict average accuracy and standard deviations for h , highlighting best/worst results by green/red arrows. Right plots show how varying α and β affect performance under different h .

Teleportation Probability α . In our push-based PPR formulation Eq. (6), α controls the balance between restarting at the source and propagating information along the bipartite graph edges. On homophilous datasets such as *Cora* and *Citeseer*, moderate values ($\alpha \approx 0.2$) effectively merge local feature overlaps with global connectivity. Conversely, for heterophilic graphs like *Squirrel*, where local neighborhoods are less reliable, a larger value ($\alpha \approx 0.5$) is

preferable to ensure that even distant yet semantically related nodes contribute to the final similarity scores.

Residual Mixing Coefficient β . Within the TEA module, Eq. (4) controls the trade-off between multi-hop aggregated features and the original node attributes. As shown in Fig. 5, in homophilous graphs such as *Cora* and *Citeseer*, the accuracy increases steadily as β rises from 0.1 to around 0.3, indicating that a moderate β effectively fuses local information with higher-order structural signals. In contrast, at $\beta = 0.5$, performance tends to plateau or even decline, suggesting that excessive residual mixing may hinder the beneficial integration of neighborhood information. Meanwhile, in the heterophilic dataset *Squirrel*, the model exhibits robust performance in a wider range of β values, although $\beta \approx 0.5$ appears to be optimal. A broader analysis of β is provided in the Supplementary Material.

Propagation Depth h . The propagation depth h determines the number of iterations over which node attributes diffuse across the graph. The bar charts (left column of Fig. 5) show that on *Cora* and *Citeseer*, setting $h = 2$ or 3 improves accuracy by approximately 2%–3% compared to $h = 0$, while increasing h beyond 3 yields diminishing returns or slight drops due to oversmoothing. A similar trend is observed on *Squirrel*, though with higher variance owing to its strongly heterophilic regions. Overall, a moderate depth of $h = 2$ or 3 is a robust default, striking a desirable balance between capturing global context and avoiding excessive smoothing.

6 Conclusion

In this paper, we introduce CoATA, a novel dual-channel GNN framework designed for Co-Augmentation of Topology and Attribute. This framework refines both topology structures and node attributes, enhancing the robustness of GNNs. Specifically, CoATA first employs the Topology-Enriched Attribute (*TEA*) module to incorporate higher-order structural information into node features, effectively mitigating issues related to noise and sparsity. Subsequently, the Attribute-Informed Topology (*AIT*) module constructs a node-attribute bipartite graph and utilizes the Personalized PageRank proximity metric to reveal multi-hop feature relationships. Following these steps, a Dual-Channel GNN aligns prototypes between

the raw and refined graphs. To validate the effectiveness of our proposed solutions, we conducted comprehensive experiments on seven real-world datasets, including five homophilic and two heterophilic graphs, comparing our approach against eleven baselines.

7 Acknowledgments

The work was supported by the National Natural Science Foundation of China 62402399. Longlong Lin and Tao Jia are the corresponding authors of this paper.

References

- [1] Reid Andersen, Fan R. K. Chung, and Kevin J. Lang. 2006. Local Graph Partitioning using PageRank Vectors. In *FOCS*.
- [2] Mehdi Azabou, Venkataramana Ganesh, Shantanu Thakoor, Chi-Heng Lin, Lakshmi Sathidevi, Ran Liu, Michal Valko, Petar Velickovic, and Eva L. Dyer. 2023. Half-Hop: A graph upsampling approach for slowing down message passing. In *ICML*.
- [3] Aleksandar Bojchevski, Johannes Gasteiger, Bryan Perozzi, Amol Kapoor, Martin Blais, Benedek Rózemerczki, Michal Lukasik, and Stephan Günnemann. 2020. Scaling graph neural networks with approximate pagerank. In *KDD*.
- [4] Deli Chen, Yankai Lin, Wei Li, Peng Li, Jie Zhou, and Xu Sun. 2020. Measuring and Relieving the Over-Smoothing Problem for Graph Neural Networks from the Topological View. In *The Thirty-Fourth AAAI Conference on Artificial Intelligence, AAAI 2020, The Thirty-Second Innovative Applications of Artificial Intelligence Conference, IAAI 2020, The Tenth AAAI Symposium on Educational Advances in Artificial Intelligence, EAAI 2020, New York, NY, USA, February 7-12, 2020*.
- [5] Ming Chen, Zhewei Wei, Bolin Ding, Yaliang Li, Ye Yuan, Xiaoyong Du, and Ji-Rong Wen. 2020. Scalable graph neural networks via bidirectional propagation. *Advances in neural information processing systems* 33 (2020), 14556–14566.
- [6] Ming Chen, Zhewei Wei, Zengfeng Huang, Bolin Ding, and Yaliang Li. 2020. Simple and Deep Graph Convolutional Networks. In *Proceedings of the 37th International Conference on Machine Learning, ICML 2020, 13-18 July 2020, Virtual Event*.
- [7] Yu Chen, Lingfei Wu, and Mohammed J. Zaki. 2020. Iterative Deep Graph Learning for Graph Neural Networks: Better and Robust Node Embeddings. In *Advances in Neural Information Processing Systems 33: Annual Conference on Neural Information Processing Systems 2020, NeurIPS 2020, December 6-12, 2020, virtual*.
- [8] Kaize Ding, Yancheng Wang, Yingzhen Yang, and Huan Liu. 2023. Eliciting Structural and Semantic Global Knowledge in Unsupervised Graph Contrastive Learning. In *Thirty-Seventh AAAI Conference on Artificial Intelligence, AAAI 2023, Thirty-Fifth Conference on Innovative Applications of Artificial Intelligence, IAAI 2023, Thirteenth Symposium on Educational Advances in Artificial Intelligence, EAAI 2023, Washington, DC, USA, February 7-14, 2023*.
- [9] Kaize Ding, Zhe Xu, Hanghang Tong, and Huan Liu. 2022. Data Augmentation for Deep Graph Learning: A Survey. *SIGKDD Explor.* 24, 2 (2022).
- [10] Kaize Ding, Chuxu Zhang, Jie Tang, Nitesh V. Chawla, and Huan Liu. 2022. Toward Graph Minimally-Supervised Learning. In *KDD '22: The 28th ACM SIGKDD Conference on Knowledge Discovery and Data Mining, Washington, DC, USA, August 14 - 18, 2022*.
- [11] Taoran Fang, Zhiqing Xiao, Chunping Wang, Jiarong Xu, Xuan Yang, and Yang Yang. 2023. DropMessage: Unifying Random Dropping for Graph Neural Networks. In *Thirty-Seventh AAAI Conference on Artificial Intelligence, AAAI 2023, Thirty-Fifth Conference on Innovative Applications of Artificial Intelligence, IAAI 2023, Thirteenth Symposium on Educational Advances in Artificial Intelligence, EAAI 2023, Washington, DC, USA, February 7-14, 2023*.
- [12] Wenzheng Feng, Yuxiao Dong, Tinglin Huang, Ziqi Yin, Xu Cheng, Evgeny Kharlamov, and Jie Tang. 2022. GRAND+: Scalable Graph Random Neural Networks. In *WWW '22: The ACM Web Conference 2022, Virtual Event, Lyon, France, April 25 - 29, 2022*.
- [13] Wenzheng Feng, Jie Zhang, Yuxiao Dong, Yu Han, Huanbo Luan, Qian Xu, Qiang Yang, Evgeny Kharlamov, and Jie Tang. 2020. Graph Random Neural Networks for Semi-Supervised Learning on Graphs. In *NeurIPS*.
- [14] Luca Franceschi, Mathias Niepert, Massimiliano Pontil, and Xiao He. 2019. Learning Discrete Structures for Graph Neural Networks.
- [15] Hongyu Guo and Yongyi Mao. 2021. Intrusion-Free Graph Mixup. *CoRR* abs/2110.09344 (2021).
- [16] Will Hamilton, Zhitao Ying, and Jure Leskovec. 2017. Inductive representation learning on large graphs. *Advances in neural information processing systems* 30 (2017).
- [17] Xiaotian Han, Zhimeng Jiang, Ninghao Liu, and Xia Hu. 2022. G-Mixup: Graph Data Augmentation for Graph Classification.
- [18] Xiangnan He, Kuan Deng, Xiang Wang, Yan Li, Yong-Dong Zhang, and Meng Wang. 2020. LightGCN: Simplifying and Powering Graph Convolution Network for Recommendation. In *SIGIR*. ACM, 639–648.
- [19] Paul W Holland, Kathryn Blackmond Laskey, and Samuel Leinhardt. 1983. Stochastic blockmodels: First steps. *Social networks* 5, 2 (1983).
- [20] Bo Jiang, Ziyang Zhang, Doudou Lin, Jin Tang, and Bin Luo. 2019. Semi-Supervised Learning With Graph Learning-Convolutional Networks. In *2019 IEEE/CVF Conference on Computer Vision and Pattern Recognition (CVPR)*.
- [21] Wei Jin, Tyler Derr, Yiqi Wang, Yao Ma, Zitao Liu, and Jiliang Tang. 2021. Node Similarity Preserving Graph Convolutional Networks. In *WSDM*.
- [22] Nikhil Varma Keetha, Chen Wang, Yuheng Qiu, Kuan Xu, and Sebastian A. Scherer. 2022. AirObject: A Temporally Evolving Graph Embedding for Object Identification. In *CVPR*.
- [23] Thomas N. Kipf and Max Welling. 2016. Variational Graph Auto-Encoders. *CoRR* abs/1611.07308 (2016).
- [24] Thomas N. Kipf and Max Welling. 2017. Semi-Supervised Classification with Graph Convolutional Networks. In *ICLR*.
- [25] Johannes Klicpera, Aleksandar Bojchevski, and Stephan Günnemann. 2019. Predict then Propagate: Graph Neural Networks meet Personalized PageRank. In *ICLR*.
- [26] Johannes Klicpera, Aleksandar Bojchevski, and Stephan Günnemann. 2019. Predict then Propagate: Graph Neural Networks meet Personalized PageRank. In *7th International Conference on Learning Representations, ICLR 2019, New Orleans, LA, USA, May 6-9, 2019*.
- [27] Xiang Li, Renyu Zhu, Yao Cheng, Caihua Shan, Siqiang Luo, Dongsheng Li, and Weining Qian. 2022. Finding Global Homophily in Graph Neural Networks When Meeting Heterophily. In *International Conference on Machine Learning, ICML 2022, 17-23 July 2022, Baltimore, Maryland, USA*.
- [28] Ziyu Liao, Tao Liu, Yue He, and Longlong Lin. 2024. Effective Temporal Graph Learning via Personalized PageRank. *Entropy* 26, 7 (2024), 588.
- [29] Longlong Lin, Yunfeng Yu, Zihao Wang, Zeli Wang, Yuying Zhao, Jin Zhao, and Tao Jia. 2024. PSNE: Efficient Spectral Sparsification Algorithms for Scaling Network Embedding. In *CIKM*. 1420–1429.
- [30] Yixin Liu, Kaize Ding, Jianling Wang, Vincent C. S. Lee, Huan Liu, and Shirui Pan. 2023. Learning Strong Graph Neural Networks with Weak Information. In *KDD 2023, Long Beach, CA, USA, August 6-10, 2023*.
- [31] Sitao Luan, Chenqing Hua, Qincheng Lu, Jiaqi Zhu, Mingde Zhao, Shuyuan Zhang, Xiao-Wen Chang, and Doina Precup. 2022. Revisiting Heterophily For Graph Neural Networks. In *Advances in Neural Information Processing Systems 35: Annual Conference on Neural Information Processing Systems 2022, NeurIPS 2022, New Orleans, LA, USA, November 28 - December 9, 2022*.
- [32] Dongsheng Yu, Wei Cheng, Wenchao Yu, Bo Zong, Jingchao Ni, Haifeng Chen, and Xiang Zhang. 2021. Learning to Drop: Robust Graph Neural Network via Topological Denoising. In *WSDM*.
- [33] Yuchen Meng, Ronghua Li, Longlong Lin, Xunkai Li, and Guoren Wang. 2024. Topology-preserving Graph Coarsening: An Elementary Collapse-based Approach. *VLDB Endow.* 17, 13 (2024), 4760–4772.
- [34] Hyeon-Jin Park, Seunghun Lee, Sihyeon Kim, Jinyoung Park, Jisu Jeong, Kyungmin Kim, Jung-Woo Ha, and Hyunwoo J. Kim. 2021. Metropolis-Hastings Data Augmentation for Graph Neural Networks. In *Advances in Neural Information Processing Systems 34: Annual Conference on Neural Information Processing Systems 2021, NeurIPS 2021, December 6-14, 2021, virtual*.
- [35] Oleg Platonov, Denis Kuznetsov, Michael Diskin, Artem Babenko, and Liudmila Prokhorenkova. 2023. A critical look at the evaluation of GNNs under heterophily: Are we really making progress? (2023).
- [36] Jiezhong Qiu, Jian Tang, Hao Ma, Yuxiao Dong, Kuansan Wang, and Jie Tang. 2018. DeepInf: Social Influence Prediction with Deep Learning. In *SIGKDD*.
- [37] Yu Rong, Wenbing Huang, Tingyang Xu, and Junzhou Huang. 2020. DropEdge: Towards Deep Graph Convolutional Networks on Node Classification. In *International Conference on Learning Representations*.
- [38] Constantin Marc Seibold, Simon Reiß, Jens Kleesiek, and Rainer Stiefelwagen. 2022. Reference-Guided Pseudo-Label Generation for Medical Semantic Segmentation. In *Thirty-Sixth AAAI Conference on Artificial Intelligence, AAAI 2022, Thirty-Fourth Conference on Innovative Applications of Artificial Intelligence, IAAI 2022, The Twelfth Symposium on Educational Advances in Artificial Intelligence, EAAI 2022 Virtual Event, February 22 - March 1, 2022*.
- [39] Prithviraj Sen, Galileo Namata, Mustafa Bilgic, Lise Getoor, Brian Gallagher, and Tina Eliassi-Rad. 2008. Collective Classification in Network Data. *AI Mag.* 29, 3 (2008).
- [40] Chao Shang, Jie Chen, and Jinbo Bi. 2021. Discrete Graph Structure Learning for Forecasting Multiple Time Series. In *9th International Conference on Learning Representations, ICLR 2021, Virtual Event, Austria, May 3-7, 2021*.
- [41] Aleksandr Shchur, Maximilian Mumme, Aleksandar Bojchevski, and Stephan Günnemann. 2018. Pitfalls of Graph Neural Network Evaluation. *CoRR* (2018).
- [42] Shantanu Thakoor, Corentin Tallec, Mohammad Gheshlaghi Azar, Mehdi Azabou, Eva L. Dyer, Rémi Munos, Petar Velickovic, and Michal Valko. 2022. Large-Scale Representation Learning on Graphs via Bootstrapping. In *The Tenth International Conference on Learning Representations, ICLR 2022, Virtual Event, April 25-29, 2022*.
- [43] Petar Veličković, Guillem Cucurull, Arantxa Casanova, Adriana Romero, Pietro Liò, and Yoshua Bengio. 2018. Graph Attention Networks. In *International Conference on Learning Representations*.
- [44] Vikas Verma, Meng Qu, Kenji Kawaguchi, Alex Lamb, Yoshua Bengio, Juho Kannala, and Jian Tang. 2021. GraphMix: Improved Training of GNNs for Semi-Supervised Learning. In *Thirty-Fifth AAAI Conference on Artificial Intelligence, AAAI 2021, Thirty-Third Conference on Innovative Applications of Artificial Intelligence, IAAI 2021, The Eleventh Symposium on Educational Advances in Artificial Intelligence, EAAI 2021, Virtual Event, February 2-9, 2021*.
- [45] Ruijia Wang, Shuai Mou, Xiao Wang, Wangepeng Xiao, Qi Ju, Chuan Shi, and Xing Xie. 2021. Graph Structure Estimation Neural Networks. In *WWW '21: The Web Conference 2021, Virtual Event / Ljubljana, Slovenia, April 19-23, 2021*.
- [46] Suhang Wang, Jiliang Tang, Charu C. Aggarwal, Yi Chang, and Huan Liu. 2017. Signed Network Embedding in Social Media. In *SIAM*.

- [47] Tongzhou Wang and Phillip Isola. 2020. Understanding Contrastive Representation Learning through Alignment and Uniformity on the Hypersphere. In *Proceedings of the 37th International Conference on Machine Learning, ICML 2020, 13-18 July 2020, Virtual Event*.
- [48] Yiwei Wang, Wei Wang, Yuxuan Liang, Yujun Cai, and Bryan Hooi. 2021. Mixup for Node and Graph Classification. In *WWW '21: The Web Conference 2021, Virtual Event / Ljubljana, Slovenia, April 19-23, 2021*.
- [49] Zeli Wang, Jian Li, Shuyin Xia, Longlong Lin, and Guoyin Wang. 2024. Text Adversarial Defense via Granular-Ball Sample Enhancement. In *ICMR*. 348–356.
- [50] Zeli Wang, Tuo Zhang, Shuyin Xia, Longlong Lin, and Guoyin Wang. 2024. GBRAIN: Combating Textual Label Noise by Granular-ball based Robust Training. In *ICMR*. 357–365.
- [51] Felix Wu, Amauri Souza, Tianyi Zhang, Christopher Fifty, Tao Yu, and Kilian Weinberger. 2019. Simplifying Graph Convolutional Networks. In *Proceedings of the 36th International Conference on Machine Learning, ICML 2019, 9-15 June 2019, Long Beach, California, USA*.
- [52] Jun Xia, Lirong Wu, Ge Wang, Jintao Chen, and Stan Z. Li. 2022. ProGCL: Rethinking Hard Negative Mining in Graph Contrastive Learning. In *International Conference on Machine Learning, ICML 2022, 17-23 July 2022, Baltimore, Maryland, USA*.
- [53] Guotong Xue, Ming Zhong, Tiejun Qian, and Jianxin Li. 2024. PSA-GNN: An augmented GNN framework with priori subgraph knowledge. *Neural Networks* 173 (2024).
- [54] Liang Yang, Zesheng Kang, Xiaochun Cao, Di Jin, Bo Yang, and Yuanfang Guo. 2019. Topology Optimization based Graph Convolutional Network. In *Proceedings of the Twenty-Eighth International Joint Conference on Artificial Intelligence, IJCAI 2019, Macao, China, August 10-16, 2019*.
- [55] Rex Ying, Ruining He, Kaifeng Chen, Pong Eksombatchai, William L. Hamilton, and Jure Leskovec. 2018. Graph Convolutional Neural Networks for Web-Scale Recommender Systems. In *SIGKDD*.
- [56] Yunfeng Yu, Longlong Lin, Qiyu Liu, Zeli Wang, Xi Ou, and Tao Jia. 2024. GSD-GNN: Generalizable and Scalable Algorithms for Decoupled Graph Neural Networks. In *ICMR*. 64–72.
- [57] Han Zhao, Xu Yang, Zhenru Wang, Erkun Yang, and Cheng Deng. 2021. Graph Debaised Contrastive Learning with Joint Representation Clustering. In *Proceedings of the Thirtieth International Joint Conference on Artificial Intelligence, IJCAI 2021, Virtual Event / Montreal, Canada, 19-27 August 2021*.
- [58] Long Zhao, Xi Peng, Yu Tian, Mubbasir Kapadia, and Dimitris N. Metaxas. 2019. Semantic Graph Convolutional Networks for 3D Human Pose Regression. In *CVPR*.
- [59] Tong Zhao, Yozen Liu, Leonardo Neves, Oliver Woodford, Meng Jiang, and Neil Shah. 2021. Data Augmentation for Graph Neural Networks.
- [60] Wentao Zhao, Qitian Wu, Chenxiao Yang, and Junchi Yan. 2024. GeoMix: Towards Geometry-Aware Data Augmentation. In *Proceedings of the 30th ACM SIGKDD Conference on Knowledge Discovery and Data Mining, KDD 2024, Barcelona, Spain, August 25-29, 2024*.
- [61] Yanqiao Zhu, Yichen Xu, Feng Yu, Qiang Liu, Shu Wu, and Liang Wang. 2020. Deep Graph Contrastive Representation Learning. *CoRR* abs/2006.04131 (2020).
- [62] Chenyi Zhuang and Qiang Ma. 2018. Dual Graph Convolutional Networks for Graph-Based Semi-Supervised Classification. In *Proceedings of the 2018 World Wide Web Conference on World Wide Web, WWW 2018, Lyon, France, April 23-27, 2018*.